









# ON AN APPROACH TO ZONING RISKS OF GROUNDWATER PROTECTIVE LAYER FAILURE BASED ON A SET OF GEOPHYSICAL AND GEOTECHNICAL CHARACTERISTICS

I. V. Losev<sup>1</sup>, A. A. Baryakh<sup>2</sup>, A. V. Evseev<sup>2</sup>, A. A. Kamaev<sup>1</sup>, I. A. Zhukova<sup>3</sup>,  
A. I. Manevich<sup>1</sup>, R. V. Shevchuk<sup>1</sup>, and D. Zh. Akmatov<sup>1</sup>

<sup>1</sup> Geophysical Center of the Russian Academy of Sciences (GC RAS), Moscow, Russia

<sup>2</sup> Mining Institute of the Ural Branch of the Russian Academy of Sciences, Perm, Russia

<sup>3</sup> PJSC "Uralkali", Berezniki, Perm Region, Russia

\* **Correspondence to:** Ilya Losev, i.losev@gcras.ru

**Abstract:** The Verkhnekamsk potassium-magnesium salt deposit (VKSD) is one of the largest in the world. The primary challenge in underground salt mining is maintaining the integrity of the groundwater protective layer, which separates the mined seams from aquifers. In this context, the Verkhnekamsk deposit is mined using a chamber system room-and-pillar method, ensuring the stability of the protective layer through inter-chamber pillars. This paper presents the results of a preliminary analysis of the geological and mining conditions in one of the mines of the Verkhnekamsk deposit. The procedure for forming the initial data set is discussed. Test calculations based on a limited data set were performed, demonstrating the potential of combining artificial neural network algorithms and discrete mathematical analysis. The results achieved on the formed dataset successfully identified hazard classes. Thus, it can be concluded that this technology is fundamentally effective for assessing the risk of groundwater protective layer failure. The proposed approach establishes links between phenomena, their associated risks, and the deformations of underground workings and the Earth's surface, enabling proactive measures to protect mines from flooding.

**Keywords:** geodynamic zoning, systems analysis, discrete mathematical analysis, groundwater protective layer, Verkhnekamsk potassium-magnesium salt deposit.

**Citation:** Losev, I. V., A. A. Baryakh, A. V. Evseev, A. A. Kamaev, I. A. Zhukova, A. I. Manevich, R. V. Shevchuk, and D. Zh. Akmatov (2025), On an Approach to Zoning Risks of Groundwater Protective Layer Failure Based on a Set of Geophysical and Geotechnical Characteristics, *Russian Journal of Earth Sciences*, 25, ES4004, EDN: SMDOXS, <https://doi.org/10.2205/2025es001015>

## 1. Introduction

The Verkhnekamsk potassium-magnesium salt deposit (VKSD) is one of the largest salt deposits in the world. The explored thickness of the potassium-magnesium salts extends over an area of 135 by 40 kilometers. The primary challenge in underground salt mining is maintaining the integrity of the rock layer located between the roof of the upper mined seam and the base of the aquifer, which is referred to as the groundwater protective layer (GWPL). A breach of the groundwater protective layer can result in underground water ingress into the mine workings, dissolution of salt rocks, and the collapse of the mine, leading to significant economic and environmental damage. Mining operations at VKSD, as well as most potassium-magnesium salt deposits, are conducted using a chamber system room-and-pillar method, leaving inter-chamber pillars to ensure the stability of the groundwater protective layer and to protect structures on the surface. However, during ore extraction, these pillars undergo deformation, resulting in the formation of subsidence troughs on the surface. All of this indicates the presence of anthropogenic stress on the layers of the groundwater protective layer and the potential risk of its integrity being compromised. For instance, out of the seven mines developed within VKSD, two (BKPRU-3

## RESEARCH ARTICLE

Received: February 19, 2025

Accepted: May 26, 2025

Published: July 3, 2025



**Copyright:** © 2025. The Authors. This article is an open access article distributed under the terms and conditions of the Creative Commons Attribution (CC BY) license (<https://creativecommons.org/licenses/by/4.0/>).

and BKPRU-1) have been flooded due to water breakthroughs in 1986 and 2006. The hazardous consequences of mine flooding also include surface subsidence, which occurs during and after the breakthrough of water into the mine workings.

Studies on the safety of mining operations at the VKSD indicate that the methods for protecting the groundwater protective layer recommended by current regulatory documents cannot be effectively implemented in the presence of “anomalous zones” within the groundwater protective layer. These are zones where geological characteristics differ significantly from those of adjacent areas of the rock mass. The work by Zubov *et al.* [2019] emphasizes that the most hazardous anomalous zones are those characterized by changes in the structure, composition, and strength properties of the groundwater protective layer rocks, including zones located above the edges of the mined-out areas. The challenge of ensuring safe mining conditions beneath the groundwater protective layer is exacerbated by the lack of complete and reliable data on the size and location of such zones during the planning stage. Several studies [Owoseni *et al.*, 2013] highlight the critical role of various mathematical methods for analyzing geospatial data in identifying such zones.

The assessment of the impact of mining operations on the groundwater protective layer is based on the observation that water-conducting fractures within the layer emerge due to the development of tensile deformations and shear stresses, which are typically concentrated at the edges of subsidence troughs [Baryakh, Gubanova, 2019]. This is a dynamically evolving process associated with the progression of mining fronts. Areas with high gradients of geological and geophysical data and their spatial-temporal distribution characteristics, such as linear features, offsets, and others, can serve as indicators of hazardous deformations and the risk of through fractures forming in the groundwater protective layer. This is analogous to the maximum subsidence values and the length of the edge part of the subsidence trough [Baryakh, Samodelkina, 2018].

Studies [Baryakh, Samodelkina, 2012; Kudryashov *et al.*, 2004] note that the prerequisites for surface subsidence following complete flooding of a mine include a combination of the following factors: a high gradient of surface subsidence (exceeding 3–4%), a weakened zone in the suprasalt layer (4–6 times reduced in strength and deformation properties), and the presence of a dissolution cavity capable of accommodating the entire volume of collapsed rock. It follows that assessing the risk of groundwater protective layer failure requires considering two groups of factors: the characteristics of structurally weakened zones (areas with increased fracturing and anisotropy, rocks with low strength properties, soluble rocks, etc.) and mining parameters along with the response of the groundwater protective layer (high-gradient zones of displacement, deformation, and stress concentration). Identifying such features based on experimental data is characterized by an unknown, multidimensional, nonlinear relationship between input and output variables.

The risks associated with deposits, including salt deposits, have been the focus of extensive research. For instance, in [Baryakh *et al.*, 2021], tests on large salt rock samples were conducted to analyze the stability of inter-chamber pillars and assess the critical rate of their transverse deformation. Another study [Baryakh, Tenison, 2021] emphasizes that one of the most critical tasks in geomechanical support of mining operations is the accurate assessment of safe mining conditions for the groundwater protective layer. Recommendations include adopting the ratio of maximum subsidence to mining depth, which is directly proportional to the slope of the Earth's surface, as a generalized criterion for defining safe mining conditions for the groundwater protective layer.

Thus, the likelihood of crack formation in the mined rock mass is associated with the presence of “anomalous” zones of two genetic types:

1. Structurally weakened areas that originally existed in the geological section (zones with increased fracturing and anisotropy, rocks with low strength properties, soluble rocks, etc.).
2. Zones of anthropogenic deformation and displacement that serve as triggers for the formation of water-conducting channels, for example, in the edge parts of subsidence troughs.

In Earth sciences, graph theory is widely used as a method of systems analysis in geoinformatics, geology, quantitative geography, and landscape ecology [Phillips *et al.*, 2015; Zhang *et al.*, 2020]. Several factors make graph theory particularly relevant to Earth sciences: the ability to work with large datasets (Big Data), its focus on spatial flows and interactions, and the growing attention to agent-based state models. Graph theory provides tools that facilitate the quantitative assessment of the properties and state of the studied natural-technical system.

One of the most powerful groups of data systems analysis methods in Earth sciences is machine learning methods and algorithms [Kolmogorov, 1957; Pedregosa *et al.*, 2012]. These are used to assess accident risks by jointly studying factors influencing the probability of occurrence, factors of environmental, population, and infrastructure vulnerability, as well as internal and external risk factors [Araujo *et al.*, 2011; Ibrahim, Bennett, 2014]. Algorithms such as Naive Bayes, Support Vector Machine,  $k$ -Nearest Neighbors, Decision Tree Bagging Random Forest, and Discriminant Analysis are utilized. The nonlinear nature of risk problems, combined with the high number of variables, justifies the use of machine learning methods to assess risk levels.

Thus, the purpose of this study is to present the results of a preliminary analysis of data from the Verkhnekamsk potassium-magnesium salt deposit using a neural network approach and the methodology of discrete mathematical analysis. Numerous examples of accidents involving water inflows into mines worldwide demonstrate that the improvement of mining methods does not entirely eliminate the possibility of surface water breakthroughs. In this regard, the development of effective methods for assessing hazards and the degree of risk of groundwater protective layer failure, along with the adoption of preventive mining measures based on these assessments, is a pressing issue for the VKSD and for salt deposits in general.

## 2. Materials and Methods

### 2.1. Methodology of Discrete Mathematical Analysis

The theoretical and practical aspects of Discrete Mathematical Analysis (DMA) for spatial data evaluation of the geodynamic hazards of structural-tectonic blocks are most comprehensively presented in the works of the Geophysical Center of the RAS [Agayan *et al.*, 2022; Gvishiani *et al.*, 2019a, 2021, 2019b]. Below, we outline their key principles. The identification of anomalous instability values within a set of geological and geophysical data fields is based on ranking the nodes of a finite two-dimensional grid to select the worst nodes. The article [Gvishiani *et al.*, 2021] introduces algorithms that account for various expert perspectives on specified functions, their properties, and dynamics, as well as on which nodes should be considered the “best”. The study employs the language of fuzzy sets and fuzzy logic, which offers significant advantages over classical sets and Boolean logic for conveying different expert interpretations of properties and processes in the geological environment. We apply this algorithm to address our zoning tasks. Assume that on the coordinate plane  $\mathbb{R}^2(x_1, x_2)$ , there is a region  $\Pi = \{a \leq x_1 \leq b; c \leq x_2 \leq d\}$ . For this region, a set of geological and geophysical fields  $\mathbf{F}$  consisting of  $m$  datasets is defined (in the form of digital maps of various parameters – geographical, geological, geophysical, geodynamic, economic, and others). The task is to evaluate the stability of the region  $\Pi$  based on the set of characteristics  $\mathbf{F}$ :

$$\mathbf{F} = \{f_1, \dots, f_m\},$$

$$f_i : \Pi \rightarrow \mathbb{R}; i = 1, \dots, m$$

or divide the region  $\Pi$  into relatively unstable (conditionally hazardous) and stable (conditionally safe) elements, i.e., effectively perform geodynamic zoning. A regular grid  $W = W(h_1, h_2)$  with nodes  $w$  is defined within the region  $\Pi$ .

$$W = \left\{ w = (a + ih_1; c + jh_2) \left| \begin{array}{l} i = 0, \dots, N; h_1 = \frac{b-a}{N} \\ j = 0, \dots, M; h_2 = \frac{d-c}{M} \end{array} \right. \right\}.$$

Next, on the grid  $W$ , it is necessary to analyze the spatial distribution of the system of functions  $F$  in the vicinity of the node  $w$ . For this purpose, a fuzzy measure of activity  $\mu_F$ , ranging from 0 to 1, is defined according to the rules described below.

*Step 1. Calculation of the Dynamic Indicator*

Each parameter  $f$  from the set  $F$  is a distribution function on the grid  $W$ . For each parameter  $f$ , a dynamic indicator  $D_f$  can be determined, which represents the functional characteristic of the measurement  $f$ . The value  $D_f(w)$  is interpreted as a quantitative assessment of the behavior of the function  $f$  at the node  $w \in W$ , calculated according to specified rules. In terms of data analysis, the dynamic indicator  $D_f(w)$  serves as a feature.

*Step 2. Calculation of the Activity Measure of the Dynamic Indicator*

For each dynamic indicator  $D_f$ , an activity measure (anomaly measure)  $\mu D_f$  is determined within the range from 0 to 1. This measure reflects the degree of expression of the property  $f$  at the node  $w$ , as defined by the indicator  $D_f$ . The activity measure  $\mu D_f$  is calculated from the dynamic indicator  $D_f$  within the framework of the discrete mathematical analysis methodology. The transition  $D_f \rightarrow \mu D_f$  transforms the analysis of the measurement  $f$  into the language of fuzzy logic: the activity measures  $\mu D_f$  for different dynamic indicators  $D_f$  are fuzzy structures on the grid  $W$  and can be combined in any configurations and quantities using fuzzy logic operations and averaging.

*Step 3. Calculation of the Integral Activity Measure  $\mu_F$*

At the final step of the algorithm, all activity measures  $\mu D_f$  are combined into a single integral indicator  $\mu_F$ . The combination formula is the arithmetic mean of all activity measures  $\mu D_f$ . Depending on the research objective, weighted coefficients for the activity measures or alternative combination formulas may be applied. To represent the measure of geodynamic safety, a value inverse to the integral activity measure is used:

$$S_F = 1 - \mu_F.$$

The transformation  $F \rightarrow \mu_F$  converts vector analysis of the system of functions  $F$  into scalar analysis of the resulting anomaly measure  $\mu$ , which, in decision-making theory, reduces a multicriteria problem to a scalar selection of a utility function. In terms of geodynamic zoning, the criteria for evaluating the value of  $S_F$  based on the set of features  $F$  are defined in Table 1. This ranking approach is appropriate, as an integral measure expressed in the range from 0 to 1 implies that conditions  $S_F \leq 0.25$  and  $S_F \geq 0.75$  indicate stability or instability, respectively. Values within the range 0.25 to 0.75 suggest uncertainty and the need for further research.

**Table 1.** Ranking of the integral measure of geodynamic safety  $S_F$

Geodynamic safety measure	Node (structural block), $S_F$
Hazardous	$\leq 0.25$
Neutral	$\in (0.25; 0.75)$
Safe	$\geq 0.75$

Thus, the algorithm includes the following parameters: 1) “Dynamic Indicator” – each dynamic indicator is interpreted as a quantitative assessment of a specific property of the initial data. 2) “Activity Measure of the Dynamic Indicator” – the measure reflects the degree of activity of the dynamic indicator on a scale from 0 to 1. 3) “Safety Measure of the Dynamic Indicator” – the value inverse to the activity measure of the dynamic indicator. 4) “Integral Safety Measure” – represents the combination of the safety measures of the dynamic indicators.

## 2.2. Formation of GIS-Oriented Database

To construct an integral safety measure applied to the problem of zoning sections of the VKSD mining fields by the degree of risk of freshwater breakthrough into mine workings, aimed at refining assessments of the risk of groundwater protective layer integrity disruption, three groups of initial data, combined into a GIS-oriented database, are used:

1. Natural characteristics (anomalies in the structure of the groundwater protective layer, depth of mining operations, effective thickness of the groundwater protective layer, physical and mechanical properties, etc.) of the geological environment and salt strata.
2. Mining-technological characteristics (number of mined seams, parameters of the mining system, extracted thickness, etc.).
3. Instrumental observation data characterizing the response of the rock mass to mining operations (convergence of mining chambers, surface deformation, collapse of the inter-seam technological layer, geophysical data, etc.).

To ensure the application of data analysis methods, it is necessary to create a consolidated data table by recording all available parameter values into a single spatial data layer. For this purpose, data layers were merged by transferring the attributes of the layers into a unified temporary data layer. Additionally, non-spatial tabular data were included in the new data layer by correlating the numbers of sections and blocks. All object features, divided into groups, were converted into numerical classes and correlated with each other.

The initial mining-technological data were supplemented with surface relief analysis data characterizing the features of the relief  $L_{Re}^1(w)$ ,  $L_{Re}^2(w)$ ,  $|\nabla_{Re}|(w)$ . The first two indicators –  $L_{Re}^1$ ,  $L_{Re}^2$ , describe geomorphological variability, while the third,  $|\nabla_{Re}|$ , represents the relief gradient. Indicators  $L_{Re}^1$ ,  $L_{Re}^2$  characterize the dissection of coordinate sections of the relief at the internal node  $w$ , both in absolute values and angular measurements [Agayan et al., 2022]. The resulting indicators are transformed into vector lines (using standard edge detection algorithms such as the Canny method and Hough transform), from which linear densities are then calculated to obtain continuously distributed parameter fields (Figure 1).

Modern tectonic movement areas are reflected not so much in height fields, curvature, and slope steepness, but in the density and depth of dissection. The terrain ruggedness index (TRI) [Migoń, Michniewicz, 2017] – a measure of vertical dissection in a given neighborhood – is considered the most appropriate for calculating dissection parameters while preserving the geomorphological meaning of the term (Figure 1a). For indicators  $L_{Re}^1(w)$ ,  $L_{Re}^2(w)$ ,  $|\nabla_{Re}|(w)$  and TRI, the arithmetic means and range (the difference between the maximum and minimum values within a section) were calculated. For subsidence data, arithmetic mean values were computed.

As a result, a single vector data layer was created, encompassing all available initial data (257 attribute fields and 1,665 data rows).

## 3. Results

As the initial data for modeling, 22 attributes were selected from 257 attribute fields based on the highest data completeness in the table and their role as the most generalized features. The selected features include groups of natural anomalies, mining-technological parameters, and instrumental observation data. Data rows with missing attribute values were removed. As a result, a dataset containing 1,615 rows was created. In the current



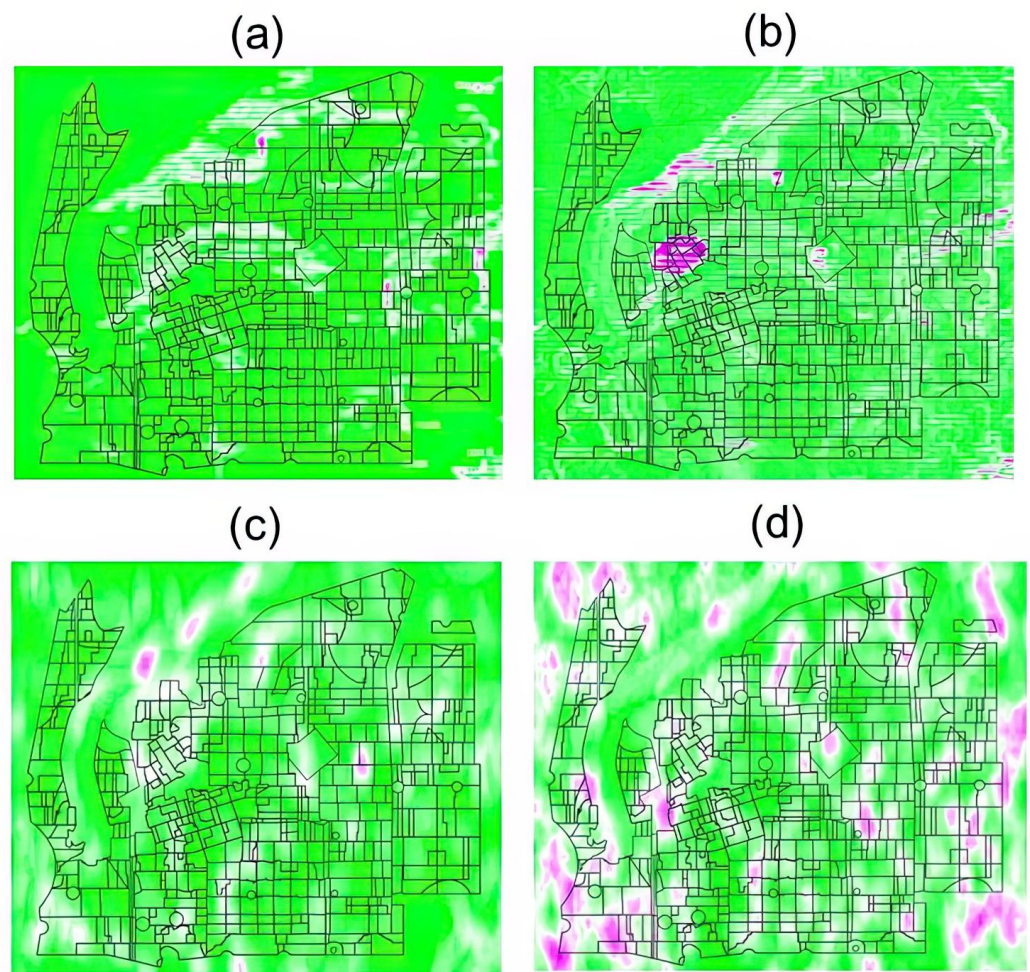


**Figure 1.** Linear Densities of Relief Indicators. a – terrain ruggedness Index; b – relief gradient  $|\nabla_{Re}(w)|$ ; c – cosine transformation, relief measure  $\mu L^1_{Re}(w)$ ; d – cosine transformation, relief measure  $\mu L^2_{Re}(w)$ .

test calculations, surface subsidence values were used as the hazard indicator. Correlation matrices and thresholds for the strength of correlation were calculated for the computed dynamic indicators  $D_f$  and their activity measures  $\mu D_f$ . The matrix includes Pearson's pairwise correlation coefficient. The lower threshold for the presence of a correlation was determined using Student's criterion (Equation 1), and the intervals for correlation strength were defined according to Equation 2:

$$r_0 = \frac{t}{\sqrt{t^2 + n - 2}}, \quad (1)$$

$$r_{\text{int}} = \frac{1 - r_0}{3}. \quad (2)$$

Thus, for the dataset used (with 1,615 rows for each indicator and a significance level of 0.95), the intervals for the strength of correlation were defined as follows:

- Weak correlation: 0.049–0.366;
- Middle correlation: 0.366–0.683;
- Strong correlation: 0.683–1.

In Figure 2, the calculated correlation matrix for 22 dynamic indicators  $\mu D_f$  is presented. The strength of the correlation is shown using a discrete color scale. Out of 231 correlation values in the initial data, 200 exhibit weak correlation. This is a positive result

from a data analysis perspective, as features should not be collinear; otherwise, high data dispersion reduces the generalization ability of the integral measure of geodynamic safety  $S_F(w)$ . The parameters of geological anomalies in group 2–4 show strong correlation due to multiple overlaps in the data. Additionally, group 2–4 has a moderate correlation with the parameter of roof depth. A moderate correlation is observed in the group of indicators related to backfill and the mining method for group 9–11. Similarly, a moderate strength of correlation exists between the TRI index and the relief indicator  $\mu L_{Re}^1(w)$ . The surface subsidence parameters within group 20–22 show strong correlation. Meanwhile, all other features demonstrate low correlation with surface subsidence, indicating an a priori lack of direct relationships between the chosen “hazard” criterion and the considered features. Subsequently, calculations were performed based on two approaches: 1 – DMA approach, involving the calculation of activity measures for the dynamic indicators  $\mu D_f$  and the integral measure of geodynamic safety; 2 – neural network approach, based on training the algorithm using the created data sample.

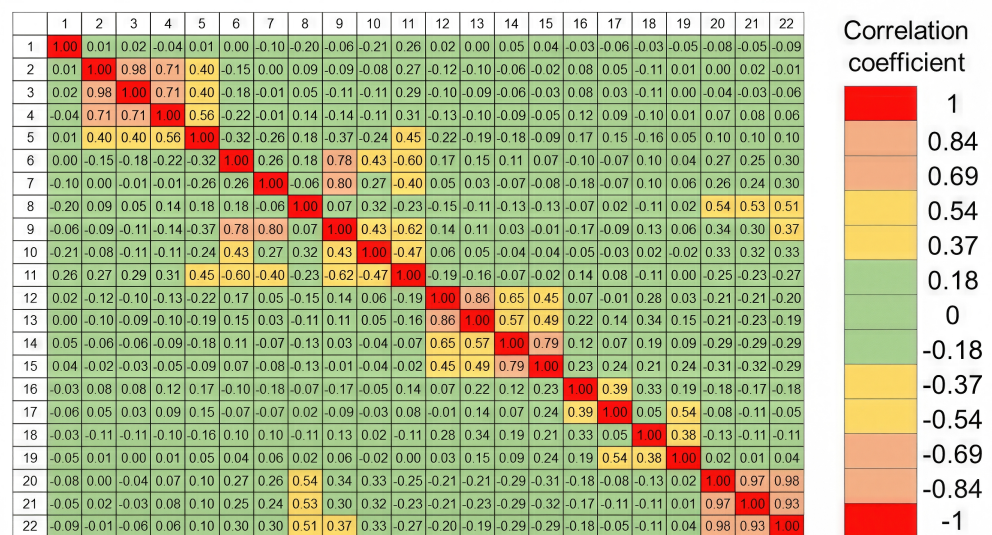


**Figure 2.** Correlation matrix of the compiled data table. 1 – mined seam; 2, 3, 4 – types of geological anomalies; 5 – roof depth; 6 – chamber width; 7 – chamber length; 8 – mining-technical load coefficient; 9 – mining-technical axial spacing coefficient; 10 – type of backfill for the mined-out space; 11 – chamber mining method; 12 – mean value of the TRI index within the section; 13 – range of TRI index values within the section; 14 – mean relief gradient  $|\nabla_{Re}(w)|$  within the section; 15 – relief gradient range  $|\nabla_{Re}(w)|$  within the section; 16 – mean value of the cosine transformation within the section, relief measure  $\mu L_{Re}^1(w)$ ; 17 – range of cosine transformation values within the section, relief measure  $\mu L_{Re}^1(w)$ ; 18 – mean value of the cosine transformation within the section, relief measure  $\mu L_{Re}^2(w)$ ; 19 – range of cosine transformation values within the section, relief measure  $\mu L_{Re}^2(w)$ ; 20 – mean value of surface subsidence within the section; 21 – minimum surface subsidence value within the section; 22 – maximum surface subsidence value within the section.

Based on the calculation of activity measures for the dynamic indicators  $\mu D_f$  of the features, the integral measure of geodynamic safety  $S_F$  was computed using DMA algorithms. In this case, two variants of the measures were calculated: one based on all the data (features 1–22) (Figure 3) and another excluding surface subsidence data (features 1–19) (Figure 4). In the case of DMA-zoning, a priori known mining-technological and geological features of the sections were not used. However, the activity measures of the dynamic indicators enable the identification of anomalous zones that correlate with geological anomaly zones.

Test calculations based on a limited dataset demonstrate the potential for the combined application of ANN algorithms and DMA. Despite the dataset's limitations, successful

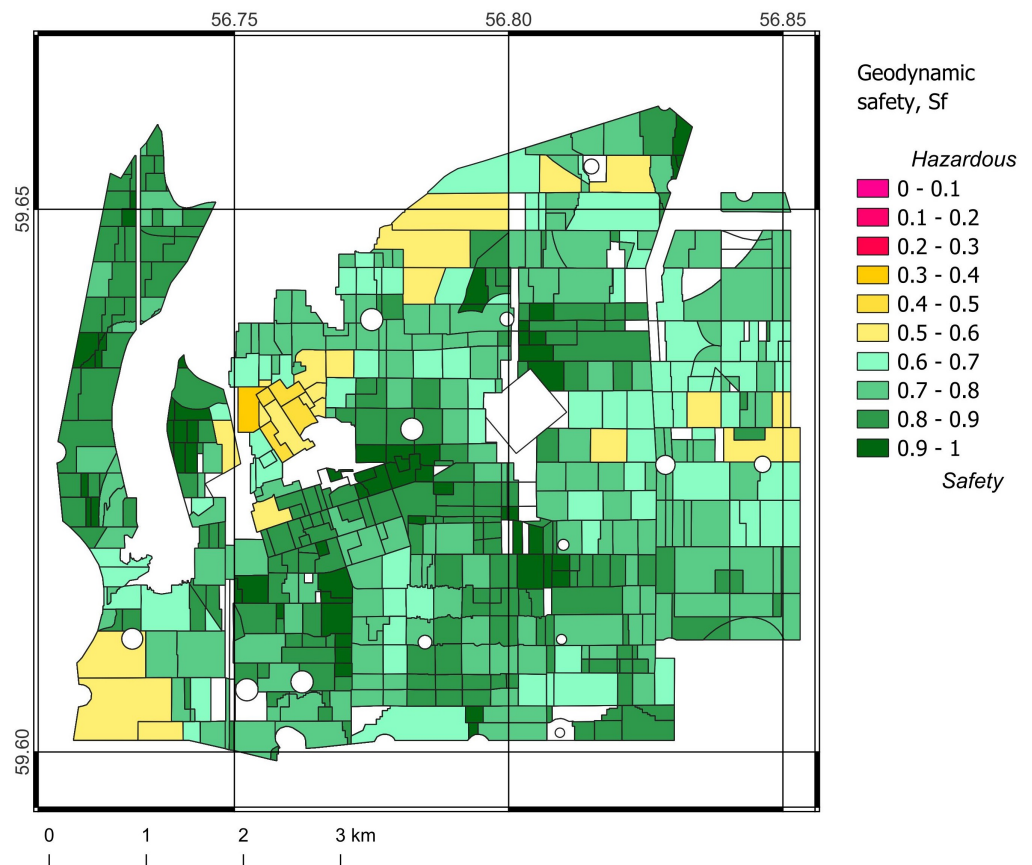


Figure 3. Geodynamic safety measure derived from all data (features 1–22, Figure 2).

results were achieved in recognizing hazard classes. This allows us to conclude that this technology is fundamentally suitable for assessing the risk of groundwater protective layer failure.

The further successful application of data analysis algorithms largely depends on the careful and detailed preparation of the initial data. This primarily concerns the choice of the “hazard” criterion. In the presented text, surface subsidence with arbitrary thresholds in millimeters was chosen as such a criterion. However, for assessing the risk of groundwater protective layer failure, a different indicator should be selected, such as section accident rates or surface deformation of the sections. To improve prediction accuracy, particular attention should be given to data collection and preparation, as well as to the geological and geophysical properties of the rock mass.

Mining-technological features, such as the year sections were first developed, mining technology, and backfill technology for mined-out spaces, show great potential for application. Using such features allows for their consideration during mine planning and enables variational hazard modeling, which helps determine optimal mining-technological parameters for resource extraction.

DMA algorithms are well complemented by ANN algorithms. Neural networks can be most effectively used for the discovery and synthesis of new recognition features and for variational calculations. As a result, the developed system (algorithm and training dataset) can be effectively trained on known data from already developed sections and applied to new areas where mining operations have not yet commenced.

#### 4. Conclusions

Systems analysis will make it possible to establish fundamental relationships between observed phenomena, their associated hazards, and recorded deformations in mine work-



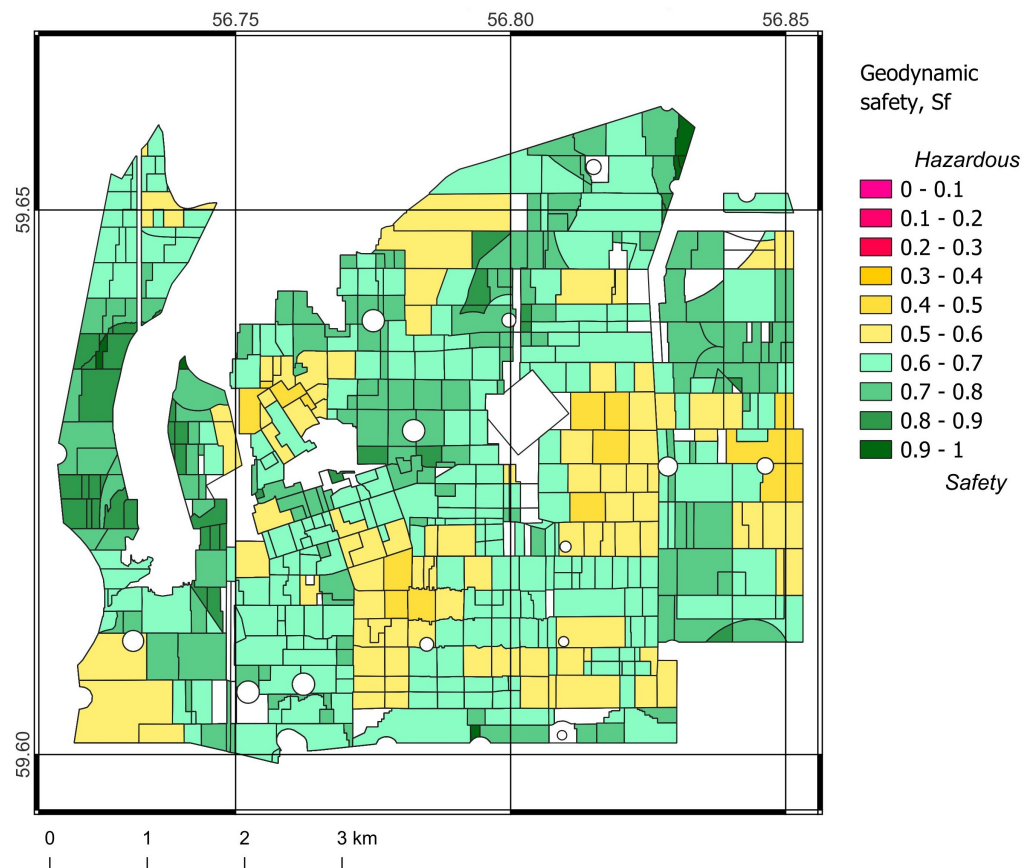


**Figure 4.** Geodynamic safety measure derived from data excluding surface subsidence (features 1–19, Figure 2).

ings and the Earth's surface. New methods and algorithms will enable the identification of hazardous anomalies in the groundwater protective layer (zones of increased gradients, linear zones, etc.), allowing for a more precise analysis of the relationship between the morphological features of the distribution of geological and geophysical parameters in the overlying strata, the geomechanical criteria for groundwater protective layer integrity disruption, and instrumentally recorded deformations of the rock mass. Frequently, the “anomalous” nature of such zones in failed stopping blocks with underground water inflows was identified only retrospectively, based on post-incident analysis. Ultimately, the causes of accidents are often attributed to ineffective protective measures, suboptimal design parameters recommended by regulatory documents, or omissions during geological exploration activities.

This will enhance the efficiency of assessing the risk of groundwater protective layer failure through the so-called emergent effect, achieved by integrating three critical components into a unified system: observations of the impact of mining operations on the groundwater protective layer, instrumental data on the state of the geological environment, and modern methods for data processing, modeling, and interpretation. A system-analytical method for assessing the risk or hazard of groundwater protective layer integrity disruption will formalize both the process of identifying anomalous hazardous zones and improve the reliability of risk assessment results. Consequently, it will also enhance the effectiveness of technical and design solutions needed to prevent such failures. Using a system-hierarchical approach to evaluate the geodynamic stability of salt rocks, the next step is to assess the stability of mine chambers, workings, and inter-chamber pillars.

In addressing this issue, the systems approach serves, on the one hand, as a tool for multifactor analysis of initial data and for the adequate formulation of scientific problems, and on the other hand, as an effective way to solve them. It helps uncover fundamental

relationships and derive new empirical dependencies between the state of inter-chamber pillars and the groundwater protective layer and the parameters of mining operations, verified by data from field geomechanical observations. Systems analysis of the interactions between individual components of the natural-technogenic system (which the groundwater protective layer itself constitutes) makes it possible to identify its properties associated with the risk of underground water breakthroughs.

**Acknowledgments.** We acknowledge this work employed facilities and data provided by the Shared Research Facility “Analytical Geomagnetic Data Center” of the Geophysical Center of RAS (<http://ckp.gcras.ru/>). This work was conducted in the framework of budgetary funding of the Geophysical Center of RAS (registration number FMWG-2025-0005) and Mining Institute of the Ural Branch RAS (registration number 124020500031-4), adopted by the Ministry of Science and Higher Education of the Russian Federation.

## References

- Agayan S. M., Losev I. V., Belov I. O., et al. Dynamic Activity Index for Feature Engineering of Geodynamic Data for Safe Underground Isolation of High-Level Radioactive Waste // *Applied Sciences*. — 2022. — Vol. 12, no. 4. — DOI: [10.3390/app12042010](https://doi.org/10.3390/app12042010).
- Araujo M., Rivas T., Giraldez E., et al. Use of machine learning techniques to analyse the risk associated with mine sludge deposits // *Mathematical and Computer Modelling*. — 2011. — Vol. 54, no. 7/8. — P. 1823–1828. — DOI: [10.1016/j.mcm.2010.11.066](https://doi.org/10.1016/j.mcm.2010.11.066).
- Baryakh A. A., Gubanova E. A. On flood protection measures for potash mines // *Journal of Mining Institute*. — 2019. — Vol. 240, no. 6. — P. 613–620. — DOI: [10.31897/pmi.2019.6.613](https://doi.org/10.31897/pmi.2019.6.613).
- Baryakh A. A., Samodelkina N. A. Water-tight stratum rupture under large-scale mining. Part II // *Journal of Mining Science*. — 2012. — Vol. 48, no. 6. — P. 954–961. — DOI: [10.1134/s1062739148060020](https://doi.org/10.1134/s1062739148060020).
- Baryakh A. A., Samodelkina N. A. Geomechanical Estimation of Deformation Intensity above the Flooded Potash Mine // *Journal of Mining Science*. — 2018. — Vol. 53, no. 4. — P. 630–642. — DOI: [10.1134/S106273911704262X](https://doi.org/10.1134/S106273911704262X).
- Baryakh A. A., Tenison L. O. Justification of engineering safety criteria for undermining of water-proof layer in the Upper Kama Salt Deposit // *Gornyi Zhurnal*. — 2021. — No. 4. — P. 57–63. — DOI: [10.17580/gzh.2021.04.08](https://doi.org/10.17580/gzh.2021.04.08). — (In Russian).
- Baryakh A. A., Tsayukov A. A., Evseev A. V., et al. Mathematical Modeling of Deformation and Failure of Salt Rock Samples // *Journal of Mining Science*. — 2021. — Vol. 57, no. 3. — P. 370–379. — DOI: [10.1134/s1062739121030029](https://doi.org/10.1134/s1062739121030029).
- Gvishiani A. D., Agayan S. M., Bogoutdinov Sh. R. Investigation of systems of real functions on two-dimensional grids using fuzzy sets // *Chebyshevskii Sbornik*. — 2019a. — Vol. 20, no. 1. — P. 94–111. — DOI: [10.22405/2226-8383-2019-20-1-94-111](https://doi.org/10.22405/2226-8383-2019-20-1-94-111). — (In Russian).
- Gvishiani A. D., Agayan S. M., Losev I. V., et al. Geodynamic hazard assessment of a structural block holding an underground radioactive waste disposal facility // *Mining informational and analytical bulletin*. — 2021. — No. 12. — P. 5–18. — DOI: [10.25018/0236\\_1493\\_2021\\_12\\_0\\_5](https://doi.org/10.25018/0236_1493_2021_12_0_5). — (In Russian).
- Gvishiani A. D., Kaftan V. I., Krasnoperov R. I., et al. Geoinformatics and Systems Analysis in Geophysics and Geodynamics // *Izvestiya, Physics of the Solid Earth*. — 2019b. — Vol. 55, no. 1. — P. 33–49. — DOI: [10.1134/s1069351319010038](https://doi.org/10.1134/s1069351319010038).
- Ibrahim A. M., Bennett B. The Assessment of Machine Learning Model Performance for Predicting Alluvial Deposits Distribution // *Procedia Computer Science*. — 2014. — Vol. 36. — P. 637–642. — DOI: [10.1016/j.procs.2014.09.067](https://doi.org/10.1016/j.procs.2014.09.067).
- Kolmogorov A. N. On the representation of continuous functions of many variables by superposition of continuous functions of one variable and addition // *Doklady Akademii Nauk SSSR*. — 1957. — Vol. 114, no. 5. — P. 953–956. — (In Russian).
- Kudryashov A. I., Vasiukov V. E., Fon-der-Flass G. S., et al. Faults on the Verkhnekamskoe deposit of salts. — Perm : Mining Institute UB RAS, Perm State University, 2004. — P. 194. — (In Russian).
- Migoń P., Michniewicz A. Topographic Wetness Index and Terrain Ruggedness Index in geomorphic characterisation of landslide terrains, on examples from the Sudetes, SW Poland // *Zeitschrift für Geomorphologie, Supplementary Issues*. — 2017. — Vol. 61, no. 2. — P. 61–80. — DOI: [10.1127/zfg\\_suppl/2016/0328](https://doi.org/10.1127/zfg_suppl/2016/0328).
- Owoseni J. O., Tamarautobou E. U., Asiwaju-Bello Y. A. Application Sequential Analysis and Geographic Information Systems for Hydrochemical Evolution Survej, Shagari Environ, Southwestern Nigeria // *Amerikan International Journal of Contemporary Reserch*. — 2013. — Vol. 3, no. 3. — P. 38–48.

- Pedregosa F., Varoquaux G., Gramfort A., et al. Scikit-learn: Machine Learning in Python // *Journal of Machine Learning Research*. — 2012. — Vol. 12. — P. 2825–2830. — DOI: [10.48550/ARXIV.1201.0490](https://doi.org/10.48550/ARXIV.1201.0490).
- Phillips J. D., Schwanghart W., Heckmann T. Graph theory in the geosciences // *Earth-Science Reviews*. — 2015. — Vol. 143. — P. 147–160. — DOI: [10.1016/j.earscirev.2015.02.002](https://doi.org/10.1016/j.earscirev.2015.02.002).
- Zhang Y., Li J., Lei Y., et al. 3D simulations of salt tectonics in the Kwanza Basin: Insights from analogue and Discrete-Element numerical modeling // *Marine and Petroleum Geology*. — 2020. — Vol. 122. — P. 104666. — DOI: [10.1016/j.marpetgeo.2020.104666](https://doi.org/10.1016/j.marpetgeo.2020.104666).
- Zubov V. P., Kovalski E. R., Antonov S. V., et al. Improving the safety of mines in developing Verkhnekamsk potassium and magnesium salts // *Mining Informational and analytical bulletin*. — 2019. — Vol. 5. — P. 22–33. — DOI: [10.25018/0236-1493-2019-05-0-22-33](https://doi.org/10.25018/0236-1493-2019-05-0-22-33). — (In Russian).